Clays Clay Miner., Vol. 70, No. 3:438–449, 2022
https://doi.org/10.1007/s42860-022-00190-9

ORIGINAL PAPER

Identification and Characterization of Nanoclays in Gamalama Volcanic Soil of Northern Maluku

I. Cipta · F. Febiyanto · A. Syoufian · I. Kartini

Accepted: 7 June 2022

Abstract Clay minerals in Gamalama volcanic soil have not yet been identified thoroughly. The soil is estimated to contain nanoscale natural clays, such as halloysite or imogolite. The occurrence of nanoclays in the soil will support the development of many applications in nanotechnologies from nature. The objective of the present study was to characterize soil samples from five different locations around the volcano at three different depths from the soil surface. A total of 50 g of dry soil sample was stirred slowly in 300 mL of distilled water. Stirring was stopped after the addition of 10 mL of 30% H_2O_2 and then allowed to stand for 24 h. The small floating particles with dimensions of <2 μm were separated from the mixture and collected using a centrifuge at 4000 rpm (1790×*g*) for 30 min. About 5 g of solid sample was obtained for further characterization. X-ray diffraction results showed the presence of halloysite, allophane, and kaolinite. Morphology analysis by scanning and transmission electron microscopy of some representative samples showed short tubes 10–20 nm in diameter and 50–100 nm long with the halloysite structure. Halloysite was found at 70 cm depth from the soil surface at almost all locations. The surface area determined by the surface area analyzer using the BET equation was as much as 112.51 m^2/g. This surface area is thought to be the largest ever determined for a natural nanoclay, paving the way for future application as catalytic or photocatalytic-supporting materials.

Keywords Allophane · Halloysite · Kaolinite · Nanoclay · Volcanic soil

I. Cipta · F. Febiyanto · A. Syoufian · I. Kartini (✉)
Department of Chemistry, Universitas Gadjah Mada, Yogyakarta, Indonesia
e-mail: indriana@ugm.ac.id

I. Cipta
Department of Chemistry Education, Universitas Khairun, Ternate, Indonesia

Introduction

Volcanic eruptions result in mineral-rich soils. As a result, soils at different locations may have different mineral compositions and physical and chemical properties. The presence of non-crystalline and crystalline clay minerals, such as allophane, imogolite, and halloysite, may result in differences in the soils. Clay minerals cover 0.84% of the earth's surface and are always found near active or inactive volcanoes.

Piedra Negras Series volcanic soil in southern Chile taken from the top 20 cm of the soil horizon was reported to contain allophane (Calabi-Floody et al., 2011). Imogolite was found to form at a depth of 100 cm in the volcanic soil of the island of Réunion, Indian Ocean (Levard et al., 2012). The mineralogical composition of volcanic soil taken from a depth of 25–105 cm at the southern foot of Mount Kilimanjaro indicates the presence of halloysite, smectite, and gibbsite (Van Ranst et al., 2020).

Indonesia has more volcanoes (>150) than any other country, scattered over almost every one of its islands (Simkin & Siebert, 1994). One of the most active

volcanoes is Mount Gamalama, located on Ternate Island, North Maluku province. Mount Gamalama has been active since 1538, leading to the creation of millions of tons of volcanic soil. Gamalama volcanic soil contains allophane with an irregular spherule shape, a diameter of 4 nm, a Si:Al ratio of 1.45, and a surface area of 125.158 m^2/g (Cipta et al., 2017). No comprehensive study of clay minerals in Gamalama volcanic soil has been carried out previously. The identification and characterization of the allophane is the only study reporting the presence of nanoclay in Gamalama volcanic soil. The present study was conducted by taking soil samples from one location with a depth of less than 30 cm from the surface. Theoretically, allophane is a metastable precursor to halloysite formation and is associated with imogolite in volcanic soils (Takahashi et al., 2001; Vacca et al., 2003).

Besides having significant agronomic potential with natural fertility, volcanic soils contain crystalline and non-crystalline clay minerals with dimensions of <2 μm (Delmelle et al., 2015). The formation of volcanic soils through weathering of volcanic glass parent materials including silicon, aluminum, and iron will form mineral products such as allophane, imogolite, or halloysite (Delmelle et al., 2015; Zehetner et al., 2003). Allophane with a globular structure is non-crystalline with the chemical formula $Al_2O_3SiO_2{\cdot}nH_2O$ and a Si/Al ratio varying from 1 to 2 (Henmi & Wada, 1976). Imogolite has the chemical formula $SiAl_2O_5{\cdot}2H_2O$ in a tube shape, 2–3 nm in diameter and several hundred micrometers long, and is associated with allophane in volcanic soils (Cradwick et al., 1972). Halloysite is a crystalline aluminosilicate clay mineral with the empirical formula $Al_2Si_2O_5(OH)_4$; it is tubular with a length of 1–2 μm, an outer diameter of 50–100 nm, and an inner diameter of 10–50 nm (Guimarães et al., 2010; Hanif et al., 2016).

According to previous studies (Calabi-Floody et al., 2011; Cipta et al., 2017; Levard et al., 2012; Takahashi et al., 2001; Vacca et al., 2003; Van Ranst et al., 2020), the Gamalama volcanic soil may also contain clay nanotubes, either halloysite or imogolite in a lower zone. The presence of halloysite or imogolite minerals in the Gamalama volcanic soil has never been studied or reported previously. The present study aimed to identify and characterize those nanotubes and other clay minerals in the volcanic soils of Mount Gamalama. The lack of information about nanoclay minerals in the Gamalama volcanic soil has meant that it is used only for plantation purposes. Information is provided here about the clay minerals in the soil and various possible nanotechnology applications are described. Applications in nanocomposite photocatalysts (Papoulis et al., 2010), adsorbance (Ramadass et al., 2019), and in medicine (Hanif et al., 2016) may be possible.

Materials and Methods

Materials

The materials used in the present study were Gamalama volcanic soil, hydrogen peroxide (H_2O_2), sodium dithionite ($Na_2S_2O_4$), sodium bicarbonate ($NaHCO_3$), sodium citrate ($Na_3C_6H_5O_7$), and double-distilled water. The chemicals were of analytical grade from Merck, Darmstadt, Germany.

Methods

Volcanic Soil Sampling

Volcanic soils were collected from five locations at three depths, 30, 70, and 100 cm below the soil surface (Fig. 1). The sampling location coordinates of samples 1, 2, 3, 4, and 5 are (0°50’12.3" N, 127°19’18.6" E), (0°50’49.6" N, 127°19’43.2" E), (0° 49’59.5" N, 127°18’44.1"E), (0°49’54.0" N, 127°18’27.1" E), and (0°49’38.9" N, 127°18’09.0" E), respectively. The soil samples were first dried for several days to remove water and facilitate grinding. After drying, all samples were ground and sieved to pass a 200 mesh sieve. Each sample was labeled according to the sampling order and depth. For example, sample 1(70) means the soil sample was from a depth of 70 cm from the soil surface at location 1.

The soil-sampling depths and locations were selected based on the FAO/UNESCO revised classification of volcanic soil (Andosol). The definition of Andosol is based on the Andic and Vitric horizons that start from 25 cm from the soil surface. Andic horizons are of two primary types, *silandic* and *alulandic*. The andic horizon where allophane and similar minerals are predominant is called the *silandic* type. The *alulandic* type is regarded as a *non-allophanic* Andosol. These two major types are found between 30 and 100 cm from the soil surface (Takahashi & Shoji, 2001). Based on that

https://doi.org/10.1007/s42860-022-00190-9 Published online by Cambridge University Press

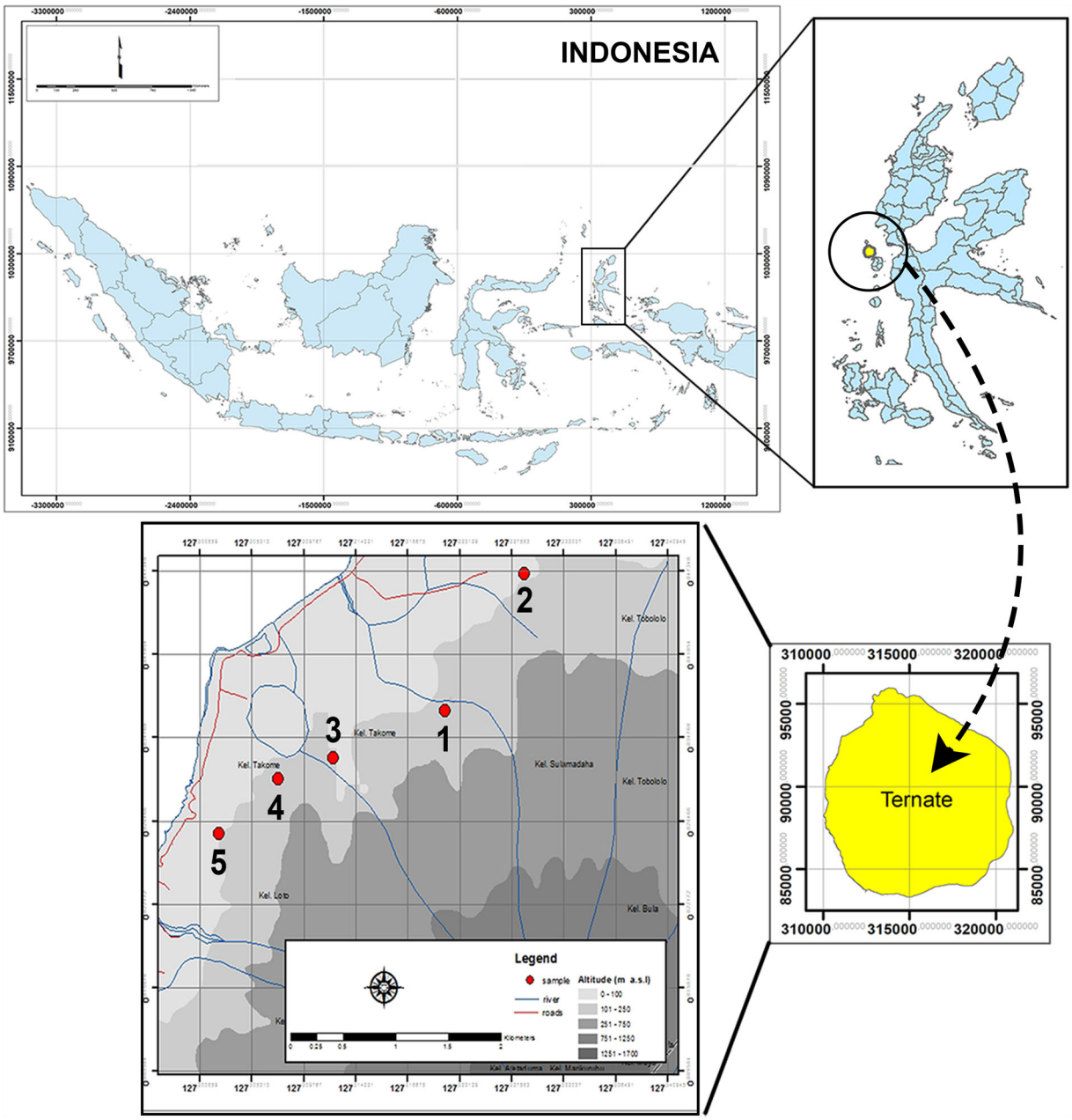

Fig. 1 Map of the locations of volcanic soil sampling at Gamalama Mt.

theory, the Gamalama volcanic soils were taken from 30, 70, and 100 cm from the soil surface at five different locations in this study.

Separation of Clay Minerals

Volcanic soil samples from Mount Gamalama were first dried at room temperature for three days. A total of 50 g of dry soil sample was dispersed in a glass beaker using 300 mL of distilled water. The soil sample was stirred slowly using a magnetic stirrer and heated at 60°C. In the process of removing the organic content, 30% H_2O_2 was added to the sample. Stirring was stopped after the addition of 10 mL of 30% H_2O_2. After 24 h, the small floating particles <2 μm in size were separated slowly from the mixture using a pipette. The colloid particles were then subjected to treatment with DCB (Dithionite Citrate Bicarbonate) to remove the organic matter and

https://doi.org/10.1007/s42860-022-00190-9 Published online by Cambridge University Press

some iron materials (Mehra & Jackson, 1958). The solid was collected using a centrifuge at 4000 rpm (1790×*g*) for 30 min (at fixed angle with 6×20 mL rotor timer control). The solid sample was then washed using 30% H_2O_2 to remove organic anions that may have been adsorbed during the DCB treatment. About 5 g of solid was then dried at room temperature for 24 h and this was continued by heating in an oven at 60°C for 2 h.

Characterization of Clay Minerals

The characterizations were done using Fourier-transform infrared spectroscopy (FTIR, Shimadzu model 8201PC, Columbia, Maryland, USA), X-ray diffractometry (XRD, Shimadzu model 6000, Columbia, Maryland, USA). scanning electron microscopy (SEM, Hitachi model SU3500, Chatsworth, California, USA), and transmission electron microscopy (TEM, JEOL model JEM 1200, Tokyo, Japan). The chemical composition was evaluated by X-ray fluorescence (XRF, Bruker model S2 Puma Series 2, Karlsruhe, Germany) and surface area analysis (Micromeritics Tristar II 3020, Norcross, Georgia, USA).).

RESULTS AND DISCUSSION

Infrared Spectra

The FTIR spectra showed similarities in the absorption peaks of each sample (Fig. 2). For example, the spectra showed significant absorption at 3448, 1635, 1033, 910, and 532 cm^{-1}. The peak at 3448 cm^{-1} indicated hydroxyl groups that may come from surface silanol, aluminol, or water (Bonelli et al., 2009). The 1635 cm^{-1} band accompanying this peak is typical of bending vibrations of H_2O (Frost et al., 2000). The Si–O–Si vibration was indicated by the absorption peak at 1033 cm^{-1} (Papoulis et al., 2010; Yuan et al., 2008). The 910 cm^{-1} band showed the Si–O–Al stretch, characteristic of Al-allophane or aluminosilicate minerals (Henmi et al., 1981). The absorption peak at 532 cm^{-1} indicated Al-octahedra, originating from the halloysite gibbsite layer (Parfitt et al., 1980). Finally, an absorption peak at 439 cm^{-1} indicated the bending vibration of Si–O–Si (Garcia-Valles et al., 2020).

The absorption pattern, especially in the 1100–900 cm^{-1} area, tended to be broader from samples from locations 1 to 5. This broadening effect was probably due to the hydrogen bonds in the sample related to the predominant clay. The presence of tubular clays, i.e. halloysite or imogolite, may increase the number of hydrogen bonds. Due to the tubular morphology, hydrogen bonding involving the outer-surface OH groups is likely (Tunega & Zaoui, 2020).

XRD Characterization

The XRD patterns revealed that halloysite exists in all of the samples tested, with various amounts of allophane and kaolinite, except for the sample from location 1 at a depth of 30 cm (Fig. 3, 1(30)). The XRD pattern of that sample showed a broad peak centered at 26.93°2θ (3.3 Å) belonging to allophane according to JCPDS No. 00-038-0449. The diffraction peaks shown by samples 1(70) and 1(100) at 8.26°2θ (10 Å), 19.69°2θ (4.5 Å), and 35.3°2θ (2.54 Å) are indicative of hydrated 10 Å-halloysite minerals, JCPDS No. 00-029-1489. Samples 1(70) and 1(100) showed a low-intensity peak of allophane, suggesting halloysite formation through allophane transformation by weathering of volcanic ash (Parfitt et al., 1983).

Samples at location 2 showed diffraction patterns dominated by kaolinite and less halloysite at increasing depth. Diffraction peaks at 21.6°2θ (4.12 Å), 23.13°2θ (3.84 Å), and 29.12°2θ (3.06 Å) correspond to the diffraction pattern data of kaolinite (JCPDS No. 01-078-2109). The halloysite diffraction peaks were observed at 19.6°2θ (4.5 Å) and 35.3°2θ (2.54 Å) for sample 2(70), according to reference JCPDS No. 00-029-1489. A diffraction peak at 27.3°2θ (3.26 Å) for sample 2 confirmed the allophane following the reference (JCPDS No. 00-038-0449).

Kaolinite minerals are present in samples 3 and 4 at various depths by the appearance of diffraction peaks at 21.6°2θ (4.12 Å), 23.13°2θ (3.84 Å), and 292θ (3.09 Å) according to JCPDS No. 01-078-2109, as well as allophane reference JCPDS No. 00-038-0449 and halloysite JCPDS No. 00-029-1489. The intensity of kaolinite and allophanes increased at deeper soil levels, while the halloysite remained constant.

Environmental conditions such as rainfall and Si concentration in the soil solution affect significantly the allophane transformation process in volcanic soils. The concentration of Si in the soil solution will decrease with increasing rainfall, indicating an increase in soil leaching (Parfitt et al., 1983). In conditions of low rainfall, the leaching process that occurs is low, causing

https://doi.org/10.1007/s42860-022-00190-9 Published online by Cambridge University Press

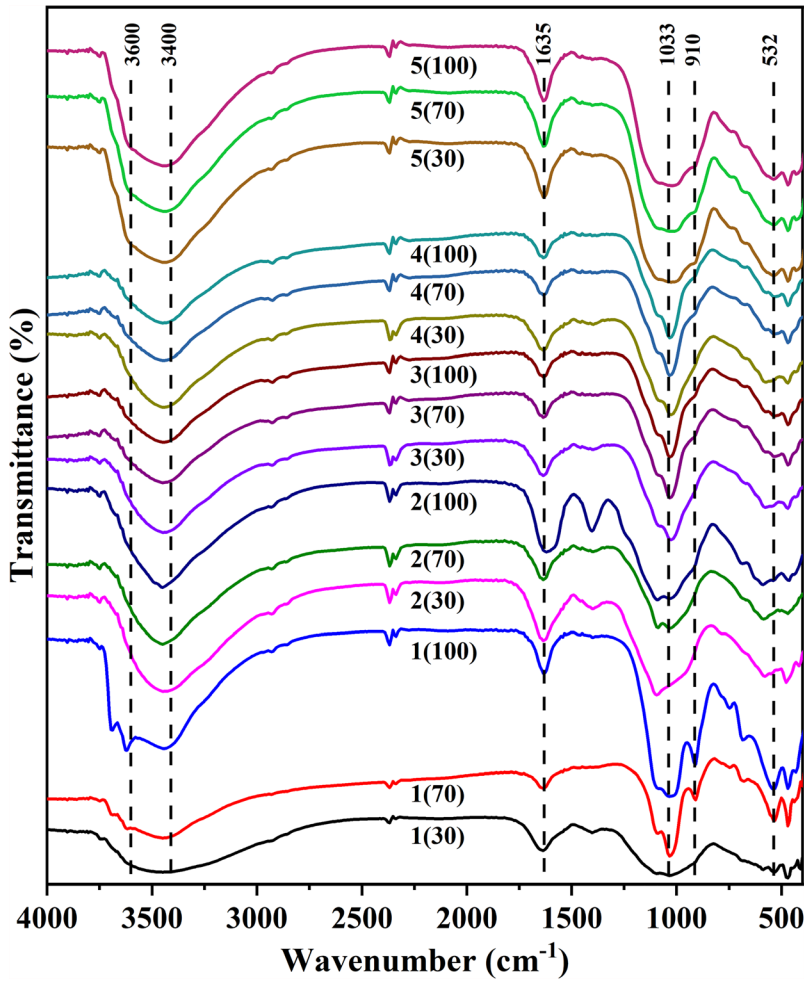

Fig. 2 FTIR spectra of Gamalama volcanic soils from five locations at three depths from the surface

the concentration of Si in the soil to be high (Harsh, 2005; Parfitt et al., 1983). According to the local Meteorology, Climatology, and Geophysical Agency, Ternate has low rainfall of ~1500 mm per year. With this paucity of rainfall, allophane tends to transform into halloysite in the Gamalama volcanic soil. Halloysite is a type of clay classified as kaolin and is usually developed early in the weathering process of volcanic soil. Halloysite is less stable than kaolinite and will transform into kaolinite over time (Huggett, 2005). The diffraction patterns in samples 3 and 4 indicated the presence of allophane, halloysite, and kaolinite. However, the kaolinite intensity increased with increasing depth. Deeper soil can be older, and the minerals in it undergo a longer weathering process. So, at increasing depth, the transformation of halloysite to kaolinite is more pronounced. Kaolinite was dominant at location 2, probably due to the longer soil formation and mineral-weathering processes than at other locations.

Samples 5 showed diffraction peaks at 19.71°2θ (4.50 Å) and 35.28°2θ (2.54 Å), indicating halloysite (JCPDS No. 00-029-1489). Allophane diffraction peaks were also observed in all samples 5, at 27.3°2θ with *d*-spacing 3.26 Å (JCPDS No. 00-038-0449), and kaolinite (JCPDS No. 01-078-2109) also. However, the intensity of allophanes tended to decrease with increasing sample depth. The minerals found in the 70 and 100 cm depth samples may have undergone a longer weathering process than those at 30 cm depth. Theoretically, weathering will cause allophane to transform into halloysite, imogolite, or kaolinite (Delmelle et al., 2015; Parfitt et al., 1983). The preferred transformation of allophane into halloysite occurs at a deeper location, however (Huggett, 2005).

https://doi.org/10.1007/s42860-022-00190-9 Published online by Cambridge University Press

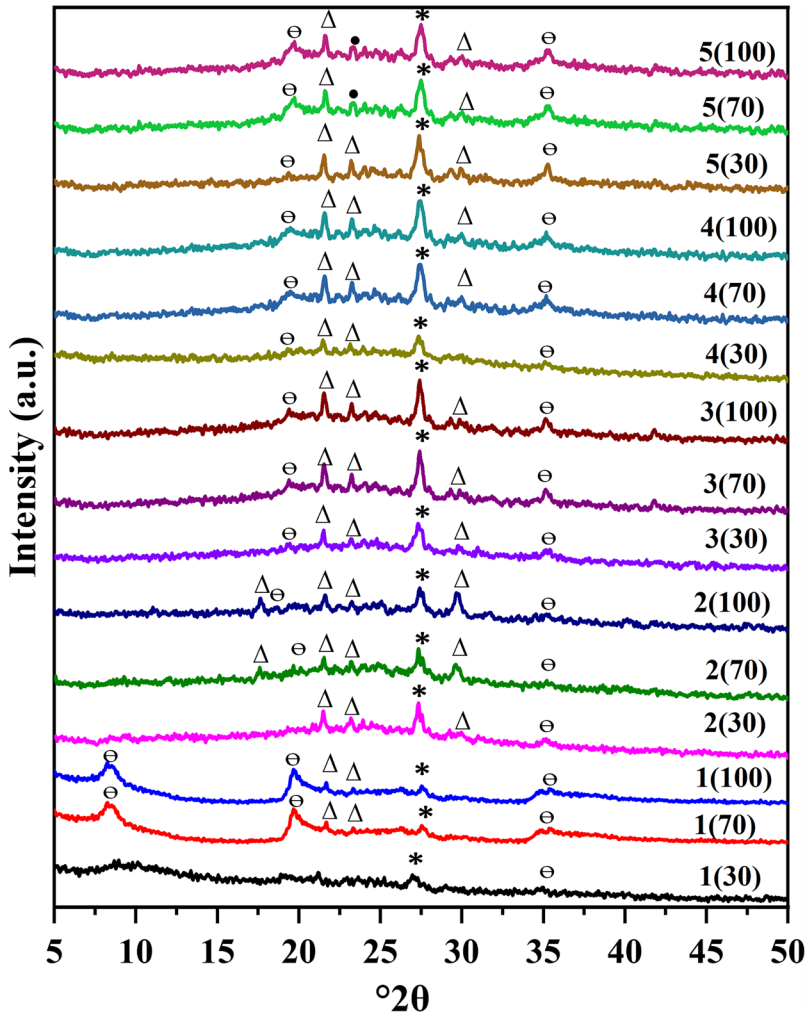

Fig. 3 XRD patterns of Gamalama volcanic soils from five locations at three depths from the surface. *: allophane; Θ: halloysite; Δ: kaolinite; •: metakaolinite

Based on the XRD patterns, one can conclude that the Gamalama volcanic soil contains allophane, halloysite, and kaolinite. Different clay minerals dominate at each location. The differences are due probably to the high and low hydration processes involved during weathering, related to the chemical dissolution of the parent volcanic material. The weathering of volcanic materials generally dissolves Si, Al, and Fe. The rate and concentration of dissolution will affect the formation of secondary minerals such as allophane, halloysite, imogolite, or kaolinite (Delmelle et al., 2015). The process of soil hydration is related to the water content of the soil, which in turn is related to the height, slope, and amount of rainfall (Gusman et al., 2018; Wahyuzi et al., 2018). The five locations have different slopes and distances from the coast, probably affecting the hydration process during weathering and causing the formation of the other minerals. However, this possibility still requires further study, such as identifying which clay minerals are present in the Gamalama volcanic soil at different heights and slopes.

SEM and TEM

Scanning (SEM) and transmission electron microscopy (TEM) were used to evaluate the morphology of the clay minerals. The mineral that dominates in each sample has a different morphology, as shown in Figs 4 and 5. Figure 4 shows spherules, stubby tubes, and plates of allophane, halloysite, and kaolinite (Bac et al., 2018;

https://doi.org/10.1007/s42860-022-00190-9 Published online by Cambridge University Press

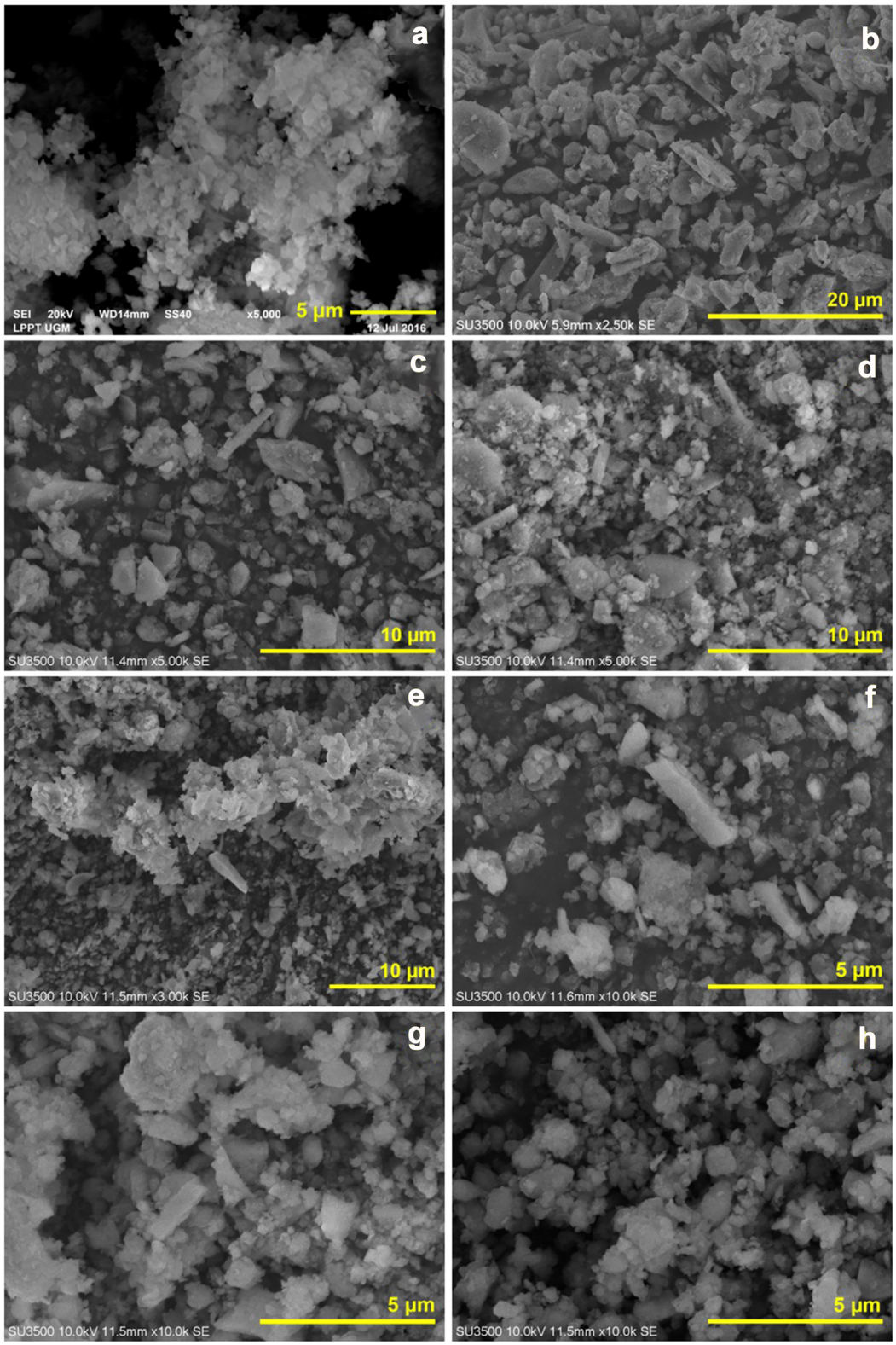

Fig. 4 SEM images of Gamalama volcanic soils: **a** 1(30), **b** 1(70), **c** 2(30), **d** 2(70), **e** 2(100), **f** 4(30), **g** 4(70), and **h** 5(70)

https://doi.org/10.1007/s42860-022-00190-9 Published online by Cambridge University Press

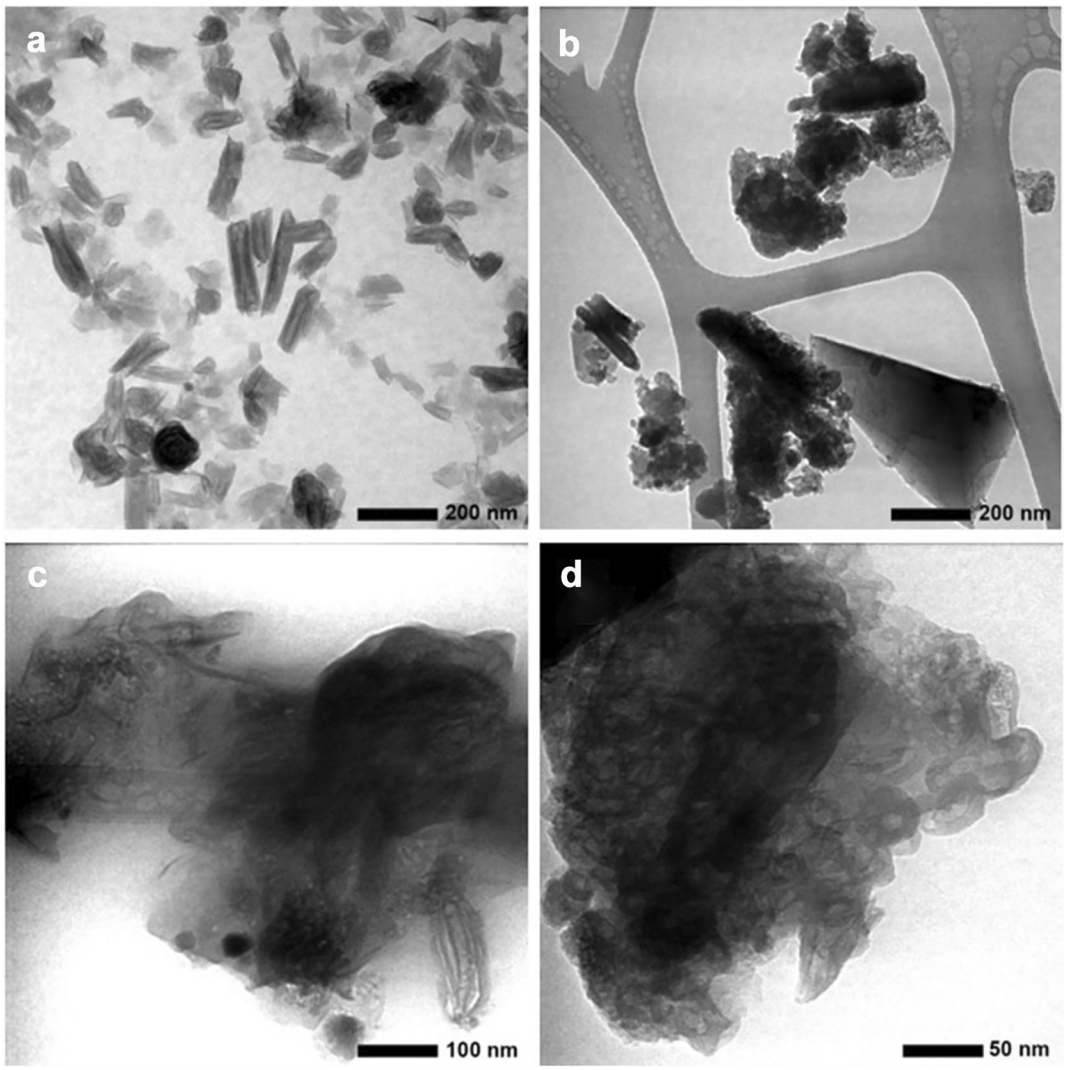

Fig. 5 TEM images of samples: **a** 1(70), **b** 2(70), **c** 4(70), and **d** 5(70)

Levard et al., 2012; Wang et al., 2020). Irregular spherules are dominant in sample 1(30), which aggregate to form a sphere diameter of ~0.1–0.5 μm. The shape of the irregular spherule is characteristic of allophane, confirming the XRD results of sample 1(30). Sample 1(70) (Fig. 4b) is dominated by the stubby porous tube shape, characteristic of halloysite. Samples 2(30) and 2(70) show the plate shape of kaolinite and irregular spherule of allophane, respectively. The kaolinite found in samples 2(30) and 2(70) has various sizes of between 1 and 3 μm. Likewise, allophane found in both samples has a variable length of between 0.1 and 0.5 μm. Samples 2(100), 4(30), 4(70), and 5(70) (Fig. 4e, f, g, h) showed the same morphological character, dominated by irregular spherules and tubes.

Transmission electron microscopy images of samples taken from four different locations at the same depth from the surface, i.e. 70 cm, are shown in Fig. 5. The TEM images corroborated both the XRD (Fig. 3) and SEM results (Fig. 4). Sample 1(70) showed that the porous tubes of halloysite dominated with diameters of 10–20 nm and lengths of ~50–100 nm. The TEM image for sample 2(70) showed an aggregated spherical morphology with a diameter of 5–10 nm, a tube shape of ~20 nm diameter, and a length of ~100 nm. The shape of the plates, typical of kaolinite, was also observed with a size of ~400 nm in this sample. The TEM images from samples 4(70) and 5(70) also showed predominant stubby porous tubes with a diameter of 20 nm and a length of 50 nm but more aggregated. The TEM images indicated

https://doi.org/10.1007/s42860-022-00190-9 Published online by Cambridge University Press

the presence of nanotube structures typical of halloysite and imogolite. The main difference between these two types of clay, apart from their XRD patterns, is the morphology. Halloysite is found naturally in spheroidal form with long, small, and stubby tubes. Natural imogolite is found in small, elongated tubes resembling fibers with a length of ~100 nm to several micrometers (Joussein et al., 2005). Based on the TEM images, one can conclude that the predominant clay mineral in Gamalama volcanic soil is halloysite. Clay minerals with different structural and morphological characters in each Gamalama volcanic soil sample may affect the surface area and the pore volume.

XRF Characterization

The chemical composition of samples from four locations at 70 cm depth showed that silica and alumina are predominant with some Fe_2O_3 (Table 1). The molar ratio SiO_2/Al_2O_3 of samples 1(70), 2(70), 4(70), and 5(70) are 1.35, 1.39, 1.46, and 1.35, respectively. The values indicate that the clay's dominant component is a 1:1 mixture, characteristic of halloysite and kaolinite (Bordeepong et al., 2011). The SiO_2/Al_2O_3 halloysite ratio in this study was similar to that found from several locations in Argentine Patagonia, which is 1.32–1.50 (Cravero et al., 2016). The existence of allophane with a Si/Al ratio >1–2 (Henmi & Wada, 1976) in all samples may also contribute to the higher SiO_2/Al_2O_3 ratio. The chemical composition revealed a high Fe_2O_3 content in halloysite (15.49 to 18.04 wt.%), which is much greater than in some of the previously reported halloysites, i.e. 1.6% (Ben M'barek Jemaï et al., 2015), 4.60% (Cravero et al., 2016), and 12.8% (Lutyński et al., 2019). The large Fe_2O_3 content found in the present study must have been the result of the high Fe content of the parent material from the Mount Gamalama eruption. Due to the significant Fe_2O_3 content, the halloysite found in Gamalama volcanic soil is probably ferro-halloysite (Ben M'barek Jemaï et al., 2015).

Specific Surface Area and Pore Size

The nitrogen adsorption-desorption method was used to determine the specific surface area and porosity. The adsorption isotherms (Fig. 6) of all selected samples were similar and followed types II and IV, indicating mesoporous material with large pore contribution. The hysteresis loop decreased with more kaolinite or allophane. The hysteresis loops may be due to the slit-shaped pores between cylindrical tubes, typically the smallest halloysite tubes. Sample 1(70) had the largest pore volume, while samples 2(70) and 4(30) were the smallest. The pore volume (Table 2) corresponded to the dominant clay phases in the sample. Samples containing predominantly halloysite showed large surface areas and pore volumes, whereas the presence of kaolinite, as detected in samples 2(70) and 4(30), resulted in small surface areas and pore volumes. The surface area was also closely related to the morphology of the material. The results of SEM and TEM images showed the predominance of stubby tube morphology in samples 1(70), 4(70), and 5(70), consistent with the large S_{BET} value. As shown in SEM and TEM images of sample 2(70) (Figs 4 and 5), the existence of the plate-shaped kaolinite may significantly reduce the surface area and pore volume.

Table 2 shows that the morphology affects the surface area, thus influencing the effectiveness of the various applications of the clays (Dong et al., 2019; Moriau et al., 2021). The largest surface areas were observed in samples 4(70) and 1(70) at 112.510 and 110.737 m^2/g, respectively. A tube-shaped halloysite dominates both samples. The surface areas of these two samples was larger than the halloysites originating from Australia,

Table 1 Chemical analysis of Gamalama volcanic soils (wt.%)

Sample	SiO_2	Al_2O_3	Fe_2O_3	MgO	CaO	Na_2O	TiO_2	SO_3	P_2O_5	K_2O
1(70)	43.82	32.28	17.45	1.27	0.92	0.88	1.63	0.31	0.55	0.36
2(70)	42.08	30.20	15.49	1.41	3.25	1.80	1.37	2.17	0.81	0.61
4(70)	44.80	30.48	16.97	1.52	2.26	0.47	1.55	0.28	0.54	0.48
5(70)	43.27	31.91	18.04	1.32	1.38	0.58	1.62	0.28	0.59	0.36

https://doi.org/10.1007/s42860-022-00190-9 Published online by Cambridge University Press

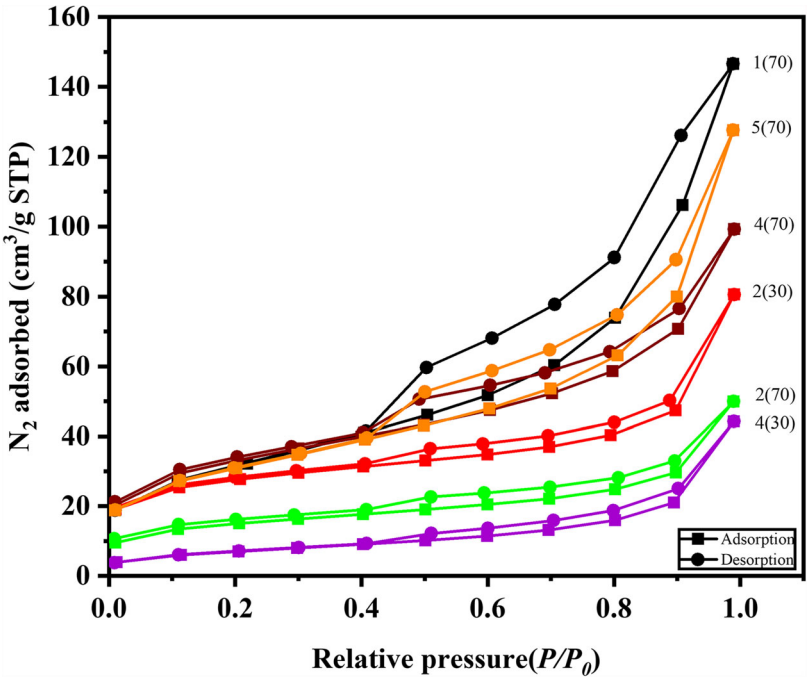

Fig. 6 Nitrogen adsorption/desorption isotherms of some samples of Gamalama volcanic soils

New Zealand, and the USA, which were reported to be 22–81 m^2/g (Pasbakhsh et al., 2013). Sample 4(30) had the smallest surface area, 24.776 m^2/g, with the smallest pore volume of 0.065 cm^3/g. Likewise, sample 2(70) had a surface area of 50.371 m^2/g.

The Gamalama volcanic soil with its halloysite content offers promise for possible use as adsorbents, supporting catalysts, or photocatalysts, due to its unique tubular structure and large surface area. Papoulis et al. (2010) revealed that natural halloysite with a surface area of 38 m^2/g increased the photocatalytic activity of TiO_2 by a factor of 3.74. Ramadass et al. (2019) reported that natural halloysite with a surface area of 50.8 adsorbs as much as 6.17 mmol/g of CO_2, more than commercial adsorbents of multi-walled carbon nanotubes (5.60 mmol/g) and mesoporous carbon nitride (5.30 mmol/g). The present authors predict that halloysites of samples 1(70) and 4(70) may result in a better performance due to their larger surface areas. Halloysite is also used as a drug carrier in drug-delivery systems due to its non-toxicity, biocompatible, high porosity, and good dispersion

Table 2 S_{BET}, pore size, and pore volume of the Gamalama volcanic soils

Sample	S_{BET} (m^2/g)	Average pore size (nm)	ǂPore volume (cm^3/g)	*Clay mineral
1(70)	110.74	8.18	0.228	Halloysite
2(30)	91.09	5.47	0.101	Allophane
2(70)	50.37	6.13	0.068	Kaolinite
4(30)	24.78	11.04	0.065	Allophane
4(70)	112.51	5.46	0.135	Halloysite
5(70)	107.19	7.37	0.186	Halloysite

ǂ BJH cumulative pore volume (adsorption branch)

* Dominant phase identified by XRD (Fig. 3)

https://doi.org/10.1007/s42860-022-00190-9 Published online by Cambridge University Press

(Kamble et al., 2012). By using the simple method employed here, halloysite can be extracted from Gamalama volcanic soil as shown by samples 1(70) and 4(70). The remaining soil can be used for a variety of purposes, including as a geopolymer material, due to the large amounts of SiO_2, Al_2O_3, and Fe_2O_3 (Zhou et al., 2022).

CONCLUSIONS

The clay minerals of the Gamalama volcanic soil from three depths at each of five locations were characterized and identified. Stubby halloysite tubes with a diameter of 10–20 nm and various lengths between 50 and 100 nm were found, especially at 70 cm. Irregular spherules of allophane and kaolinite plates were also observed. The surface area of the soil samples was between 24.7763 and 112.51 m^2/g depending on the location. A large surface area was observed in samples that were dominated by halloysite. Applications for adsorption and supporting materials for catalysts or photocatalysts are envisaged for Gamalama volcanic soils.

Acknowledgments The authors gratefully acknowledge financial support by a Universitas Gadjah Mada RTA Grant 2020.

Author Contribution Conceptualization and final writing: Indriana Kartini
Writing – original draft preparation: Indra Cipta
Supervision: Indriana Kartini, Akhmad Syoufian
Data processing: Febiyanto

Funding Universitas Gadjah Mada through RTA Grant 2020.

Data availability The datasets generated during and/or analyzed during the current study are available from the corresponding author on reasonable request.

Declarations

Research Involving Human Participants and/or Animals This study did not involve any human or animal participants.

Conflicts of interest The authors declare that they have no conflict of interest concerning the study in this paper.

References

Bac, B., Dung, N., Khang, L., Hung, K., Lam, N., An, D., … Tinh, B. (2018). Distribution and Characteristics of Nanotubular Halloysites in the Thach Khoan Area, Phu Tho, Vietnam. *Minerals, 8*(7), 290–302.

Ben M'barek Jemaï, M., Sdiri, A., Errais, E., Duplay, J., Ben Saleh, I., Zagrarni, M. F., & Bouaziz, S. (2015). Characterization of the Ain Khemouda halloysite (western Tunisia) for ceramic industry. *Journal of African Earth Sciences, 111*, 194–201.

Bonelli, B., Bottero, I., Ballarini, N., Passeri, S., Cavani, F., & Garrone, E. (2009). IR spectroscopic and catalytic characterization of the acidity of imogolite-based systems. *Journal of Catalysis, 264*(1), 15–30.

Bordeepong, S., Bhongsuwan, D., Pungrassami, T., & Bhongsuwan, T. (2011). Characterization of halloysite from Thung Yai District. *Journal of Science and Technology, 33*, 599–607.

Calabi-Floody, M., Bendall, J. S., Jara, A. A., Welland, M. E., Theng, B. K. G., Rumpel, C., & Mora, M. de la L. (2011). Nanoclays from an Andisol: Extraction, properties and carbon stabilization. *Geoderma, 161*(3–4), 159–167.

Cipta, I., Limatahu, N. A., Nur Abu, S. H., Kartini, I., & Arryanto, Y. (2017). Characterization of allophane from Gamalama volcanic soil, North Maluku, Indonesia. *Asian Journal of Chemistry, 29*(8), 1702–1704.

Cradwick, P. D. G., Farmer, V. C., Russel, J. D., Masson, C. R., Wada, K., & Yoshinaga, N. (1972). Imogolite, a Hydrated Aluminium Silicate of Tubular Structure. *Nature Physical Science, 240*(104), 187–189.

Cravero, F., Fernández, L., Marfil, S., Sánchez, M., Maiza, P., & Martínez, A. (2016). Spheroidal halloysites from Patagonia, Argentina: Some aspects of their formation and applications. *Applied Clay Science, 131*, 48–58.

Delmelle, P., Opfergelt, S., Cornelis, J.-T., & Ping, C.-L. (2015). Volcanic Soils. In *The Encyclopedia of Volcanoes* (2nd ed.). Elsevier.

Dong, F., Meng, Y., Han, W., Zhao, H., & Tang, Z. (2019). Morphology effects on surface chemical properties and lattice defects of Cu/CeO_2 catalysts applied for low-temperature CO oxidation. *Scientific Reports, 9*(1), 12056.

Frost, R. L., Kristof, J., Horvath, E., & Kloprogge, J. T. (2000). Rehydration and phase changes of potassium acetate-intercalated halloysite at 298 K. *Journal of Colloid and Interface Science, 226*(2), 318–327.

Garcia-Valles, M., Alfonso, P., Martínez, S., & Roca, N. (2020). Mineralogical and thermal characterization of kaolinitic clays from Terra Alta (Catalonia, Spain). *Minerals, 10*(2), 142–156.

Guimarães, L., Enyashin, A. N., Seifert, G., & Duarte, H. A. (2010). Structural, electronic, and mechanical properties of single-walled halloysite nanotube models. *Journal of Physical Chemistry C, 114*(26), 11358–11363.

Gusman, M., Nazki, A., & Putra, R. R. (2018). The modelling influence of water content to mechanical parameter of soil in analysis of slope stability. *Journal of Physics: Conference Series, 1008*(1), 012022.

Hanif, M., Jabbar, F., Sharif, S., Abbas, G., Farooq, A., & Aziz, M. (2016). Halloysite nanotubes as a new drug-delivery system: a review. *Clay Minerals, 51*, 469–477.

Henmi, T., Tange, K., Minagawa, T., & Yoshinaga, N. (1981). Effect of SiO_2/Al_2O_3 ratio on the thermal reactions of allophane. II. Infrared and x-ray powder diffraction data. *Clays and Clay Minerals, 29*, 124–128.

Henmi, T., & Wada, K. (1976). Morphology and composition of allophane. *American Mineralogist, 61*, 379–390.

Harsh, J. (2005). Amorphous Materials. In *Encyclopedia of Soils in the Environment* (pp. 64–71). Elsevier.

Huggett, J. M. (2005). Clay Minerals. In *Encyclopedia of Geology* (pp. 358–365). Elsevier.

Joussein, E., Petit, S., Churchman, J., Theng, B., Righi, D., & Delvaux, B. (2005). Halloysite clay minerals – a review. *Clay Minerals, 40*, 383–426.

Kamble, R., Ghag, M., Gaikawad, S., & Panda, B. K. (2012). Halloysite nanotubes and applications: a review. *Journal of Advanced Scientific Research, 3*, 25–29.

Levard, C., Doelsch, E., Basile-Doelsch, I., Abidin, Z., Miche, H., Masion, A., … Bottero, J. Y. (2012). Structure and distribution of allophanes, imogolite and proto-imogolite in volcanic soils. *Geoderma, 183–184*, 100–108.

Lutyński, M., Sakiewicz, P., & Lutyńska, S. (2019). Characterization of diatomaceous earth and halloysite resources of Poland. *Minerals, 9*, 670–686.

Mehra, O. P., & Jackson, M. L. (1958). Iron oxide removal from soils and clays by a dithionite–citrate system buffered with sodium bicarbonate. *Clays and Clay Minerals, 7*, 317–327.

Moriau, L., Bele, M., Marinko, Ž., Ruiz-Zepeda, F., Koderman Podboršek, G., Šala, M., … Suhadolnik, L. (2021). Effect of the Morphology of the High-Surface-Area Support on the Performance of the Oxygen-Evolution Reaction for Iridium Nanoparticles. *ACS Catalysis, 11*(2), 670–681.

Papoulis, D., Komarneni, S., Nikolopoulou, A., Tsolis-Katagas, P., Panagiotaras, D., Kacandes, H. G., … Katsuki, H. (2010). Palygorskite- and Halloysite-TiO_2 nanocomposites: Synthesis and photocatalytic activity. *Applied Clay Science, 50*, 118–124.

Parfitt, R. L., Furkert, R. J., & Henmi, T. (1980). Identification and structure of two types of allophane from volcanic ash soils and tephra. *Clays and Clay Minerals, 28*, 328–334.

Parfitt, R. L., Russell, M., & Orbell, G. E. (1983). Weathering sequence of soils from volcanic ash involving allophane and halloysite, New Zealand. *Geoderma, 29*, 41–57. https://doi.org/10.1016/0016-7061(83)90029-0

Pasbakhsh, P., Churchman, G. J., & Keeling, J. L. (2013). Characterization of properties of various halloysites relevant to their use as nanotubes and microfibre fillers. *Applied Clay Science, 74*, 47–57.

Ramadass, K., Singh, G., Lakhi, K. S., Benzigar, M. R., Yang, J. H., Kim, S., … Vinu, A. (2019). Halloysite nanotubes: Novel and eco-friendly adsorbents for high-pressure CO_2 capture. *Microporous and Mesoporous Materials, 277*, 229–236.

Simkin, T., & Siebert, L. (1994). Volcanoes of Indonesia. In *Volcano Discovery* (p. 349). Springer Netherlands.

Takahashi, T., Dahlgren, R. A., Theng, B. K. G., Whitton, J. S., & Soma, M. (2001). Potassium-Selective, Halloysite-Rich Soils Formed in Volcanic Materials from Northern California. *Soil Science Society of America Journal, 65*, 516–526.

Takahashi, T., & Shoji, S. (2001). Distribution and classification of volcanic ash soil. *Global Environmental Research, 6*, 83–96.

Tunega, D., & Zaoui, A. (2020). Mechanical and Bonding Behaviors behind the Bending Mechanism of Kaolinite Clay Layers. *Journal of Physical Chemistry C, 124*, 7432–7440.

Vacca, A., Adamo, P., Pigna, M., & Violante, P. (2003). Genesis of Tephra-derived Soils from the Roccamonfina Volcano, South-Central Italy. *Soil Science Society of America Journal, 207*, 198–207.

Van Ranst, E., Kips, P., Mbogoni, J., Mees, F., Dumon, M., & Delvaux, B. (2020). Halloysite-smectite mixed-layered clay in fluvio-volcanic soils at the southern foot of Mount Kilimanjaro, Tanzania. *Geoderma, 375*, 114527–114539.

Wahyuzi, R., Zakaria, Z., & Sophian, R. I. (2018). Slope stability affected by percentage of soil water content in Dago Giri, West Bandung regency. *AIP Conference Proceedings, 1987*(1), 020030.

Wang, X., Cheng, H., Chai, P., Bian, J., Wang, X., Liu, Y., & Pan, Z. (2020). Pore Characterization of Different Clay Minerals and Its Impact on Methane Adsorption Capacity. *Energy & Fuels, 34*, 12204–12214.

Yuan, P., Southon, P. D., Liu, Z., Green, M. E. R., Hook, J. M., Antill, S. J., & Kepert, C. J. (2008). Functionalization of halloysite clay nanotubes by grafting with γ-aminopropyltriethoxysilane. *Journal of Physical Chemistry C, 112*, 15742–15751.

Zehetner, F., Miller, W. P., & West, L. T. (2003). Pedogenesis of Volcanic Ash Soils in Andean Ecuador. *Soil Science Society of America Journal, 67*, 1797–1809.

Zhou, S., Zhu, X., Lu, C., & Li, F. (2022). Synthesis and characterization of geopolymer from lunar regolith simulant based on natural volcanic scoria. *Chinese Journal of Aeronautics, 35*, 144–159.